Effect of intermixing on bulk and interface Raman modes in GaAs:AlAs superlattice waveguide structures

P. Scrutton, B. Fung, and A. S. Helmy[a]
Edward S. Rogers Sr. Department of Electrical & Computer Engineering, University of Toronto, Toronto, Ontario M5S 3G4, Canada

(Received 2 June 2008; accepted 31 July 2008; published online 1 October 2008)

Spatially resolved Raman spectroscopy at room temperature is used to study quantum well intermixing in GaAs:AlAs superlattice structures. Phonon modes are probed from the side facet along the [110] direction. The intermixing leads to the appearance of interfacial alloy modes and degraded the intensity of the superlattice interface (IF) modes, which can be used as a sensitive indicator of superlattice quality. These changes in the Raman spectra, along with spatially resolved photoluminescence, are used to distinguish the degree of intermixing in samples intermixed by impurity free vacancy diffusion at 850–950 °C, and to investigate the bandgap modulation in a periodically intermixed bandgap grating fabricated using ion implantation induced disordering. The shift of the GaAs-transverse optic mode to the GaAs-like transverse optic alloy mode and the degradation of the GaAs-IF mode are shown to provide the best indication of the extent of intermixing. Due to the large contrast in the GaAs-IF mode intensity between as-grown and intermixed superlattice, using IF modes is found to be a promising route for characterizing the resolution of the superlattice bandgap grating. © *2008 American Institute of Physics*.
[DOI: 10.1063/1.2986149]

I. INTRODUCTION

Photonic devices based on ultrafast nonlinear optical effects in compound semiconductors offer unique advantages over their counterparts using carrier-based nonlinearities. Advantages over popular optical materials such as ferroelectrics, bulk crystals, and dielectrics include higher nonlinear coefficients, mature fabrication technology, and the capability of stronger light localization through nanostructuring. Out of the numerous alternatives offered by compound semiconductors, short period superlattice (SL) structures have emerged as an attractive platform for devices based on nonlinear optical effects. Waveguides with a core made out of SL structures offer a range of benefits over those with a core made out of multiple quantum wells or bulk compound semiconductors. The control over the electronic properties attained in SL structures tailors the resonant components of nonlinear optical tensors including $\chi^{(2)}$ and $\chi^{(3)}$ more effectively than their multiple quantum well counterparts.[1] For optimum device functionality, spatial control over these nonlinear effects and hence the bandgap of these SL structures is necessary. Lateral control on the order of the wavelength of operation entails an approximate lateral resolution <1 μm.[2,3] While the bandgap can be controlled using numerous technologies, one of the postgrowth techniques that has demonstrated immense promise is quantum well intermixing (QWI). QWI technologies have evolved to become a strong candidate for the realization of photonic integrated circuits. These technologies are now widely applied for the fabrication of devices such as optical switching matrices and for laser diodes integrated with passive sections such as gratings and external cavities.[4]

[a]Electronic mail: a.helmy@utoronto.ca.

Modulation of the third-order susceptibility coefficient $\chi^{(3)}$ has been investigated for all optical switching devices with improved performance over their bulk counterparts.[2] One of the main metrics of enhancing the efficiency of all optical switches based on soliton emission is the interface between the highly nonlinear and the nominally linear regions. In essence, the IF region defines the transfer function of these switches and hence needs to be studied carefully. Devices made in GaAs/AlGaAs multiple quantum well structures have been demonstrated recently, with incomplete switching taking place.[2] By using SL structures instead of quantum wells, the modulation in the nonlinearity will be enhanced, as has been demonstrated recently.[1] However, optimization of the interface region has not yet been carried out and is bound to pose substantial influence on the device figure of merit. An effective means to resolve the bandgap within the linear/nonlinear transition is necessary.

Similarly, modulation of the resonant component of the second-order susceptibility coefficient $\chi^{(2)}$ in periodically intermixed SL structures has been used to enable quasi-phase-matching (QPM).[3] To achieve QPM for wavelengths around 1.55 μm, first order bandgap gratings with periods on the order of 3 μm are necessary. The principle has recently been implemented in GaAs:AlAs SL structures[5] where QPM was enabled by the periodic modulation of $\chi^{(2)}$.[6] The measured efficiency was, however, lower than predicted. This is likely to be due to limitations posed by the QWI process used, fabrication imperfections, and scattering from the unavoidable refractive index grating generated in conjunction with the bandgap grating.[5]

A reliable, informative and rapid nondestructive characterization technique is needed to aid in the optimization and design of the aforementioned applications, where the preci-

0021-8979/2008/104(7)/073103/9/$23.00 © 2008 American Institute of Physics

Author complimentary copy. Redistribution subject to AIP license or copyright, see http://jap.aip.org/jap/copyright.jsp

sion of the spatial bandgap modulation is an important parameter governing the device performance. Optical measurements including reflection, transmission, and luminescence are commonly used to provide information nondestructively on bandgap grating structures. In particular, spatially resolved photoluminescence (PL) is commonly used to observe bandgap modulations. However, PL resolution is intrinsically limited by the diffusion length of the excited carriers prior to their recombination, which is on the order of 1 μm in GaAs.[7] Consequently, there is a lower limit on the size of the period that can be studied and on the sharpness of the interface between bandgap regions that can be detected. Sharp modulation between the regions of different bandgap is important to achieve efficient functionality in the applications discussed above.[8] For this reason, characterization by Raman spectroscopy offers an important advantage over PL. The Raman signal does not depend on carrier recombination and hence improves on the spatial resolution. For structures with varying bandgaps with feature sizes on the order of 1–2 μm or smaller, this superior resolution can be crucial.

Besides offering improved spatial resolution, Raman spectroscopy also provides information that cannot be obtained from PL. The lattice vibrations probed by the Raman process are very sensitive to their local environment in the lattice. As such, shifts in the peak wave numbers, peak widths, and changes in their relative strengths can indicate variations in lattice order and stress.[7] It can also be used for chemical profiling.[9] Further, quantum-confined heterostructures, particularly SL structures, have unique phonon modes that appear in the Raman spectra and these have been thoroughly studied for GaAs:AlAs SL. These include zone-folded acoustic phonons, confined optical phonons (COPs), and electrostatic interface (IF) phonon modes.[10] Shifts in the longitudinal COP modes have been previously used to study QWI in GaAs:AlAs SL,[11,12] however these studies used a backscattering [001] configuration. In SL core devices, the SL layer will often be buried under cladding, cap, or contact layers and the SL will not be accessible from the [001] direction. Therefore in devices where the SL is not in the surface vicinity, probing is usually carried out along the side-facet or [110] direction from which the longitudinal optical (LO) modes are not observed. It should also be noted that bulk Raman modes of the lattice have been used previously to characterize intermixing.[13,14] However, the modulation in the bulk Raman modes offers a limited compositional dispersion and hence provide limited signal to noise ratio (SNR) when investigating compositional intermixing.

In this work, spatially resolved Raman spectroscopy obtained through probing the SL structure along the [110] direction is used to study as grown and intermixed waveguides with a SL core. The effect of intermixing on the Raman modes observed, particularly the IF modes, is compared to theoretical predictions. Correlation between the PL peak shift and the Raman modes' evolution is also discussed. Finally, the characterization of bandgap gratings which were used to achieve domain disordering for QPM is illustrated.

II. EXPERIMENTAL DETAILS

The wafer structure used in this study is comprised of a 600 nm 14:14 GaAs:AlAs core layer grown with [001] orientation between a 1.1 μm upper cladding and a 4.3 μm lower cladding of $Al_{0.6}Ga_{0.4}As$. A 100 nm GaAs cap layer was deposited on top. The details of the structure were published previously.[6] In order to avoid absorption in the GaAs cap layer at the probe wavelength and hence improve the SNR of the Raman signal from the SL core, the measurements were carried out along the samples side facet. As such, the laser beam is incident on the [110] plane of freshly cleaved sample. Conducting the measurements on a freshly cleaved surface avoids signal degradation due to oxide formation. According to the Raman selection rules, the phonons observed in this configuration will be transverse optic (TO) modes and these will have wave vector components parallel to the SL IFs.[10]

Several samples originating from the GaAs:AlAs SL structure were systematically examined using Raman spectroscopy, including as-grown (sample 1) and nominally fully intermixed SL (sample 2) samples. Sample 2 was intermixed by 4 MeV As^+ ion implantation with a dose of 2×10^{13} ions/cm^2 and subsequent rapid thermal annealing at 850 °C for 30 s. These conditions have been obtained through the optimization of the intermixing process to maximize the amount of intermixing while minimizing the implantation induced damage, which leads to excessive optical losses.[6,14] Complete intermixing of the SL core in sample 2 is expected to result in an $Al_{0.5}Ga_{0.5}As$ layer. The Raman spectra from samples 1 and 2 were then compared with the spectra from samples intermixed to varying degrees. The intermixing was carried out by impurity-free vacancy diffusion (IFVD) using large area SiO_2 caps and rapid annealing at temperatures between 750 and 950 °C (samples 3–7). The annealing process had a ramp up rate of 50 °C s^{-1} followed by a ramp down of 50 °C s^{-1}. The silica layer used was a spin-on glass, deposited to a thickness of ~380 nm, and cured at a temperature of 400 °C for 2 h. Finally periodically intermixed SL core structure (sample 8), which was produced using the same ion-implantation procedure as sample 2 with a periodic gold mask of 1.5 μm thickness, was examined. The samples details are compiled in Table I. A transport of ions in matter software (TRIM) simulation predicted that As^+ energy of 4 MeV would correspond to an ion range of 1.7 μm and a lateral straggle of 0.45 μm, which are adequate for the creation of group III vacancies in the SL while the desired spatial resolution is maintained.[6] The incident ion beam was tilted by ±7 to prevent channeling effects that would increase the damage incurred. The role of the Au mask thickness of ~1.5 μm was confirmed by simulations to be sufficient to protect the desired regions from the As^+ ions.[14]

Raman and PL Measurements were carried out at room temperature with a Jobin–Yvon Horiba LabRAM micro-Raman system using a continuous wave (cw) 532 nm frequency-doubled Nd:YAG (yttrium aluminum garnet) laser. An excitation laser power of 1.8 mW was focused through a 100× objective. The spectrometer had a

Author complimentary copy. Redistribution subject to AIP license or copyright, see http://jap.aip.org/jap/copyright.jsp

TABLE I. The SL core samples.

Sample	Intermixing	Annealing
1	None	None
2	As^{+} ion implantation with 2×10^{13} ions/cm^2	30 s at 850 °C
3	IFVD with 380 nm SiO_2 caps	750 °C (50 °C/s ramp up/down)
4	IFVD with 380 nm SiO_2 caps	800 °C (50 °C/s ramp up/down)
5	IFVD with 380 nm SiO_2 caps	850 °C (50 °C/s ramp up/down)
6	IFVD with 380 nm SiO_2 caps	900 °C (50 °C/s ramp up/down)
7	IFVD with 380 nm SiO_2 caps	950 °C (50 °C/s ramp up/down)
8	As^{+} ion implantation with 2×10^{13} ions/cm^2 and a 1.5 μm thick periodic gold mask	30 s at 850 °C

1200 g mm^{-1} grating and a spectral resolution of 2.4 cm^{-1} pixel^{-1}. The incident light was polarized in a transverse electric (TE) configuration, with the electric field polarized along the SL layers. This polarization provides maximum SNR because it optimally couples with the TO modes.[10] While the spatial scans were carried using a xy-stage with a step size of 0.1 μm, the spatial resolution is limited by the spot size of the incident beam. The numerical aperture of the objective used is 0.9. At the operating wavelength, the diffraction limited spot size is on the order of the wavelength used, which compares well with the features studied in this work (2–5 μm). In order to obtain the coordinates of the SL within the vertical structure, the intensity of the Raman modes pertinent to the SL are monitored while the laser is scanned orthogonal to the epitaxial layers starting from the substrate toward the surface. The point where the SL Raman modes are maximal is where the laser spot is placed for the lateral scan across the intermixed domains.

To consider the effect of the finite optical beam on the features obtained from the lateral scans across the intermixed domains, the Gaussian spot of the laser probe with the appropriate size should be deconvolved from the profiles obtained through the Raman mode scans. This would provide the actual shape of the intermixed regions.

Using the edge-on geometry lends itself to facile depth profiling along the growth direction. This allows more freedom with the selection of laser wavelength, as absorption in the upper layers will not degrade the signal obtained. The drawback of this geometry is that the TO modes of the SL layer are closely spaced in wavenumber to those of the cladding layers and will overlap in the collected spectra. The PL spectra were fit with a single asymmetrical Gaussian peak and the Raman spectra were fit with mixed Gaussian–Lorentzian peaks.

III. PHONON DISPERSION MODELS

In this section, the theoretical predictions of phonon modes in SL structures will be reviewed. This will provide a foundation on which the sample analysis and subsequent interpretations will be based. There are two commonly used basic models which describe phonon modes in SL structures. Those are the mechanical model and the dielectric continuum model.

The mechanical or linear chain model assumes that the confined LO and TO modes are described by a nearest neighbor linear chain model using the bulk force constants.[15] The model only predicts modes vibrating perpendicular to the SL layers, along the growth direction. TO modes have negligible angular dispersion in this model due to weak coupling with the electrostatic potential. Therefore these modes correspond well to the in-plane modes.[16] For the 14:14 SL we study here, the linear chain model predicts that the COP dispersion is essentially the bulk dispersion folded such that each band becomes a set of 14 modes at the zone center. In the GaAs TO range, the total spread, in wave numbers, of the COP modes is <12 cm^{-1}, with a maximum spacing between adjacent modes of only 1.2 cm^{-1}. Due to this limited TO dispersion and finite mode widths, the COP modes are expected to overlap in wave number. The predicted mode intensities also drop quickly with increasing order.[10]

The dielectric continuum model takes into account the electrostatic effects. The material is described by its bulk dielectric constant and Maxwell's equations are applied.[17] The polarization discontinuity at IFs in III-V SL structures leads to finite surface charge densities and exponentially attenuating electric fields, which couple together and interact with the polar optical phonons causing IF modes to evolve from the LO and TO bulk frequencies. These polariton modes have maxima near the IFs, however, the modes of all the IFs are coupled, producing a collective excitation of the SL.[16,17] This model predicts pairs of GaAs-like and AlAs-like IF polariton bands.[10,17] These bands evolve from the TO and LO mode frequencies at the [001] direction and meet for equal GaAs and AlAs layer widths halfway between these frequencies at the orthogonal [110] direction.[17]

Both models only predict a part of the behavior of phonon modes in SL structure. They fall short of taking into account that the mechanically confined modes and the IF modes will couple through the electrostatic potential.[18] Continuum models can be derived, where both electrostatic and mechanical boundary conditions are fulfilled, in which phonon modes are treated as hybrids of LO, TO, and IF modes.[19] This model was developed for GaAs:AlAs SL,[20] where a complete set of optical phonon modes in the range between the bulk LO and TO modes is predicted with an accuracy comparable to more complicated three-dimensional lattice dynamics calculations.[20,21] This model has been termed the phenomenological continuum model.

Author complimentary copy. Redistribution subject to AIP license or copyright, see http://jap.aip.org/jap/copyright.jsp

TABLE II. Observed Raman peaks for the SL core samples.

Sample	Peak designation	Position (cm^{-1})	Expected position[a] (cm^{-1})
SL layer	GaAs-TO [IF]	267 [278, 284]	268 [277, 282, 284][b]
In as-grown	AlAs-TO	360	360.1
sample	AlAs-IF/LO	380.5	382.5[c]
SL layer	GaAs-like TO	260.4	360.0 (50% Al)
In intermixed	AlAs-like TO	359.4	260.8 (50% Al)
sample	AlAs-like LO	383.6	385.9 (50% Al)
$Al_{0.6}Ga_{0.4}As$	GaAs-like TO	259.1	259.5
Cladding in	AlAs-like TO	360.4	360.1
Intermixed and as-grown samples	AlAs-like LO	386.6	389.6

[a]Fit to empirical equations in Ref. 23.
[b]Calculation with phenomenological continuum model of Ref. 20.
[c]Dielectric continuum model of Ref. 17.

A. Modes prediction from the phenomenological continuum model

In our structure, the SL is cladded with $Al_{0.6}Ga_{0.4}As$ layers, and so the SL modes discussed above will arise alongside alloy modes in the Raman spectra. In $Al_xGa_{1-x}As$ alloy, both GaAs-like and AlAs-like LO and TO bands arise.[22] Extensive investigations on $Al_xGa_{1-x}As$ with a large number of precisely known Al compositions were carried out previously.[23] Alloying also introduces atomic disorder to the lattice, which causes an asymmetric broadening of the phonon bands and leads to the appearance of disorder activated (DA) modes around 245 cm^{-1} (GaAs-like) and 380 cm^{-1} (AlAs-like).[23] In addition, with a 532 nm probe, a sharp increase in the integrated mode intensity occurs near $x=0.7$ for all modes due to resonant enhancement as the E_0 bandgap energy aligns with the probe wavelength. The SL bandgap is further away from the probe wavelength than the cladding bandgap, and the corresponding scattering intensity is weaker on the SL.

Given the growth direction and the GaAs substrate orientation, the SL growth direction [001] translates to the Γ-(Δ)-X dispersion. It is this direction that will be folded due to the extended SL period. Full bulk dispersions for GaAs and AlAs have been calculated previously along [001].[24] The TO (LO) bands take on zone center and edge values of 271 and 254 cm^{-1} (291 and 240 cm^{-1}) in GaAs and 363 and 337 cm^{-1} (400 and 393 cm^{-1}) in AlAs. These will be compared with the Raman modes measured in this work in the next section. The TO bands and the AlAs LO band have limited dispersion, while the GaAs LO dispersion is the greatest. Also, the LO-TO splitting is much greater for AlAs. Zone folding of these bands and the creation of gaps leads to sets of confined modes with virtually no dispersion.[10]

Interactions between the IF and COP modes are taken into account in the phenomenological continuum model. This is necessary to accurately predict the phonon wavenumber near the GaAs IF band. The model has successfully predicted mode mixing and anticrossings of the LO and TO modes with the IF modes with angular dispersion.[20] The calculated phonon frequencies near the GaAs IF bands for an in plane wave vector corresponding to an edge directed 532 nm probe are given in Table II. The values used for v_L and v_T were obtained by Zunke *et al.*,[21] and take the values of $\varepsilon_0=12.4$ and $\varepsilon_\infty=10.6$ in GaAs, and $\varepsilon_0=10.1$ and $\varepsilon_\infty=8.2$ in AlAs. Penetration of the GaAs vibrations into the AlAs barriers was accounted for by increasing the effective GaAs well width by a monolayer at the expense of the AlAs layer.

B. Quantum well intermixing effects on phonon modes

QWI will have several effects on the phonons in the SL. Cationic intermixing will create regions of $Al_xGa_{1-x}As$ alloy. The presence of these alloy layers at layer interfaces will lead to the appearance of GaAs-like and AlAs-like alloy modes, as discussed above. As the composition varies over the interface, a range of alloy mode frequencies will arise. The structural disorder associated with these layers will lead to the appearance of DA modes. Due to the relatively small volume they occupy within the measurement volume, the strength of these modes is likely to be substantially smaller than those of the SL layers. The LO alloy modes in these interfacial layers may couple with the polariton bands to contribute to the in-plane spectra, and the TO alloy modes will overlap with the GaAs and AlAs bulklike TO features. This will all contribute to the Raman spectra collected.[11]

The continuum model showed that in a GaAs/AlAs SL, it is the mixing of the confined LO phonons with the polariton bands that gives rise to the sharp GaAs IF modes in our spectra. As such a decay in confined LO mode intensity will mean a decrease in IF mode intensity. However, only slight decreases in the confined LO phonon intensities are usually seen.[11] Meanwhile, the polariton bands will also be affected by the reduced dielectric/bandgap modulation. This means weaker electron confinement and less surface charge at the interfaces to contribute to the electrostatic potential. Ultimately the IF modes are expected to disappear with substantial intermixing. The Raman intensity is proportional to the polarization field generated by the optical phonons. This polarization is related to the electronic susceptibility χ. It has been shown that both the $\chi^{(2)}$ and $\chi^{(3)}$ coefficients substantially decrease with QWI.[25] Chamberlain extended the continuum model referred to above to obtain an expression for

Author complimentary copy. Redistribution subject to AIP license or copyright, see http://jap.aip.org/jap/copyright.jsp

the IF-like mixed mode scattering intensity in ideal GaAs/AlAs SL,[26] starting with an equation for the induced polarization field of a phonon, $p_i^{\text{ind}}=\Sigma_j \chi_j E_j'^{I}$, where $\chi_j=\Sigma_l b E_l^*$, E_l^* is the electric field of the phonon and $E_j'^{I}$ is the incident light field. Here ignoring geometric factors and the Bose–Einstein thermal factor, the following relation was obtained:

$$I \propto b^2 \frac{16\varepsilon}{(\varepsilon^2+1)^4} R_{zz},$$

where R_{zz} is the Raman cross section and depends on the layers widths, phonon wavevectors, and effective charges. To a first approximation, the b^2 term is proportional to the square of $\chi^{(2)}$, and thus the IF mode scattering intensity is roughly proportional to the square of the second order susceptibility. As such, the IF mode signal is expected to weaken dramatically with intermixing.

The lower dielectric contrast at the interfaces also serves to reduce the splitting of the polariton bands, which is proportional to $\Delta\varepsilon$. This may however be obscured due to broadening as the IF bands couple to the interfacial alloy modes.[10]

Structural disorder, which may allow a wider range of wave vectors to become active in scattering, will also broaden the Raman features. We can estimate the IF-LO mixed-mode dispersion with QWI by using the continuum model.[20] In its derivation, the model assumed that the mechanical dispersion of the IF modes with changing well thickness was negligible. As such we assume that the modulation of the dielectric profile with intermixing has a much weaker effect on the phonon dispersion than the change in well width.

IV. MEASUREMENTS

In order to predict the effect of intermixing on the mode behavior, the width of the GaAs region of the SL is reduced, while keeping the dielectric modulation and the period unaffected in the phenomenological continuum model. It was found that trends in the edge dispersion are difficult to discern. However, anticrossings between the IF and confined LO modes generally move to lower wave numbers for small reductions in the GaAs layer width. This is primarily due to the decrease in frequency with well width that is seen in the linear chain model.[20] In addition, by reducing the dielectric modulation in this model, it was found that even for large reductions in $\Delta\varepsilon$, the phonon wave numbers exhibited very small shifts [with respect to the modes full width at half maximum (FWHM)]. For example, with a decrease to half the initial dielectric mismatch, the IF mode at 280 cm^{-1} at the in-plane direction shifted down less than 1 cm^{-1} in our 14:14 SL. These observations support the assertion that the decrease in IF mode intensity should be a stronger indicator of intermixing than any other shifts in this mode range.

A. Nonpatterned as-grown and fully intermixed samples

First, the fully intermixed and as-grown samples (samples 1 and 2) are studied to serve as a reference. Raman and PL profiles were taken across the SL along the [001] direction. The SL region is easily identified in the Raman scans due to the large decrease in Raman scattering intensity relative to the cladding. This reduction is due to the lower index of refraction on the SL and to the reduced resonance effects, where the bandgap of the SL layer is further away from the pump laser in comparison to that of the cladding. The SL room temperature PL wavelength was 752 nm for TE polarization, and 732 for TM. These values match those predicted by the band structure calculations for this structure.[27] The samples exhibit numerous Raman modes. The dominant peaks appearing in the Raman spectra are compiled in Table II. Representative spectra from the as-grown and fully intermixed SL and from $Al_{0.6}Ga_{0.4}As$ cladding are shown in Fig. 1. From the spectra, the similarity between Raman spectra of the intermixed SL and those of the $Al_{0.6}Ga_{0.4}As$ alloy is evident. The similarity is consistent with the expectation that the fully intermixed SL is similar to $Al_{0.5}Ga_{0.5}As$ alloy.

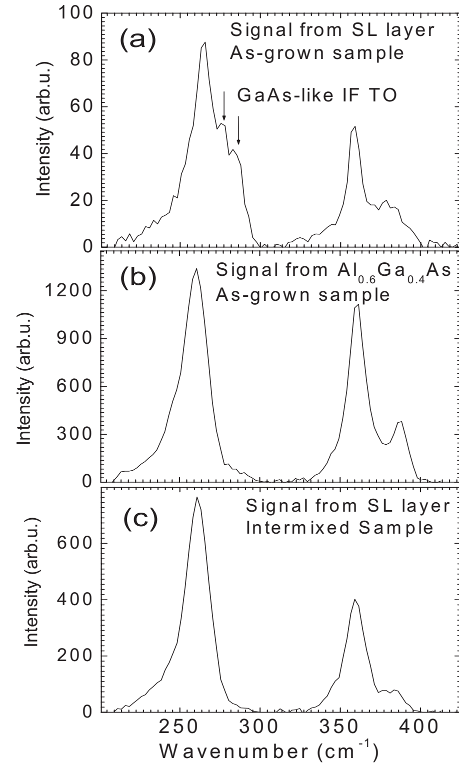

FIG. 1. Raman spectra are shown from (a) the SL layer and (b) the $Al_{0.6}Ga_{0.4}As$ cladding in the as-grown sample, and from (c) the SL layer in the intermixed sample.

The Raman mode with the lowest wave number is observed at 260 cm^{-1} for the fully intermixed layer and at 267 cm^{-1} in the intact SL. These peaks are identified as those of the GaAs-TO alloy mode and the GaAs-TO mode originating in the GaAs layers in the SL, respectively. Evidence of confined TO modes for the as-grown SL was not resolved, consistent with expectations due to the limited TO dispersion.

The mode at 360 cm^{-1} is identified as that of the AlAs-TO mode of the AlAs available in the as-grown SL. It can also arise from the AlAs-like TO alloy mode for the intermixed SL and for the $Al_{0.6}Ga_{0.4}As$ alloy. The AlAs-TO mode features limited dispersion across the Brillouin zone (BZ) (Ref. 24) and negligible dispersion with varying Al

Author complimentary copy. Redistribution subject to AIP license or copyright, see http://jap.aip.org/jap/copyright.jsp

content in the alloy.[23] As such no significant shift in this peak is seen for any of the spectra. However, the peak FWHM decreases notably on the as-grown SL. This is consistent with greater order in the AlAs SL layers in comparison to the alloy.

The Raman mode with the highest wave number, in the vicinity of 390 cm^{-1}, is identified as that of the AlAs-like LO mode for the $Al_{0.6}Ga_{0.4}As$ cladding. It can also arise from the intermixed SL, in which case it is observed as a broad feature relating to the AlAs-IF modes in the as-grown SL. This feature for intact SL structures has been observed in previous SL studies,[17] and corresponds to the predictions of the dielectric continuum model. On the intermixed SL, the peak appears 3 cm^{-1} lower than on the $Al_{0.6}Ga_{0.4}As$ alloy, which compares well with the 4 cm^{-1} shift predicted for a change in Al fraction from 50% to 60%.[23]

The most interesting feature of the comparison of the SL Raman spectra between the intact and intermixed SL is the appearance of Raman modes at 278 and 284 cm^{-1}. These modes correspond well with the GaAs-IF modes predicted by dielectric and phenomenological continuum models, as discussed in the previous section.[17,20] They were observed previously in Raman scattering studies of intact GaAs/AlAs SL structures.[17,21] Their presence is a clear indication of quality of the as-grown SL. Under nonresonant conditions, these modes will only arise for Raman pump polarization aligned with the in-plane growth direction of the epitaxial layers.[21]

Comparing the contrast in Raman features for intact and intermixed SL it is clear that the 6 cm^{-1} shift of the GaAs-TO mode is much larger than that exhibited by the two AlAs-like modes. However, the appearance of the GaAs-IF modes only on the as-grown sample demonstrates that these modes are the strongest indicator of SL quality in the Raman spectra. The two samples studied in this section will serve as reference points to study samples intermixed to different extent as well as periodically intermixed samples, where we aim to periodically intermix the SL to render the region effectively bulk $Al_{0.5}Ga_{0.5}As$. However, the intermediate states of intermixing are also of great interest because they shed light on the sensitivity of this technique to detect and quantify the intermediate intermixing states that may exist on the boundaries of the different domains in bandgap grating structures. These will be the regions between the intermixed and unintermixed domains. During the analysis of IFVD intermixed and the periodically intermixed samples, focus will be placed on the GaAs-TO and GaAs-IF modes.

B. Nonpatterned samples with varying degree of intermixing

Raman and PL measurements were carried out in the center of the SL layers of samples 3–7 to examine the evolution of the optical properties of the SL layer with intermixing. The PL is examined first to provide a clear indication of the degree of intermixing through the bandgap shift. The PL wavelength peak in the SL region is plotted versus annealing temperature in Fig. 2. The peak wavelength decreases with increasing the annealing temperature at similar rates for both TE and TM polarization. It is evident from the figure that for

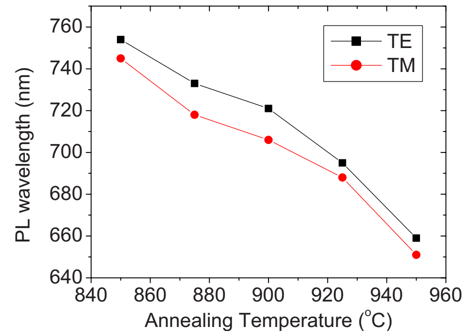

FIG. 2. (Color online) Raman spectra on the IFVD intermixed SL samples annealed at 850–950 °C.

the annealing temperature of 850 °C, minimal intermixing of 6 and 2 nm has taken place for the TE and TM modes, respectively.[27] While at the annealing temperature of for the 950 °C, the amount of intermixing observed does not correspond to complete intermixing, leading to an AlGaAs alloy.[27]

Raman spectra obtained from samples 3–7 are shown in Fig. 3. The parameters of the corresponding Raman features, including peak position, FWHM, and intensity are compiled in Table III. Some trends are evident in the Raman modes with increasing annealing temperature as can be seen in Fig. 3.

- The relative intensity of the GaAs-like IF modes decrease monotonically with annealing temperature. They ultimately became indistinguishable from the TO mode.
- The GaAs-like TO mode downshifts in wave number as the alloy fraction increases with annealing temperature.
- The AlAs-like TO mode shows no notable peak shift due to its negligible dispersion with composition, but a moderate increase in the FWHM occurs with annealing temperature and hence intermixing.
- The highest Raman peak shows an evolution from the AlAs IF mode to the AlAs-like LO mode. This is clearest for the samples annealed at 925 and 950 °C, where the relative peak intensity increases as expected for the LO alloy mode versus the IF mode.

In spite of these trends, it would be constructive to quantify the Raman modes behavior with annealing temperature,

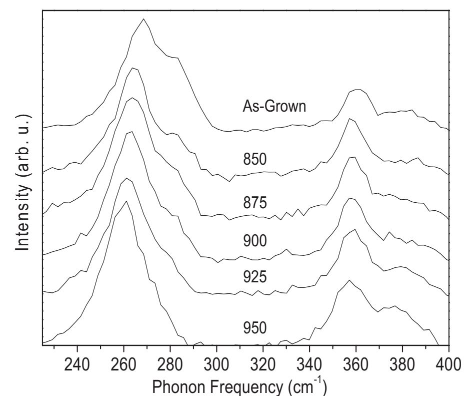

FIG. 3. PL peak position at the center of the SL vs annealing temperature.

Author complimentary copy. Redistribution subject to AIP license or copyright, see http://jap.aip.org/jap/copyright.jsp

TABLE III. Raman spectral parameters

Annealing temperature (°C)	GaAs-like TO mode Peak (cm^{-1})	FWHM (cm^{-1})	Intensity (arbitrary units)	GaAs IF mode Peak (cm^{-1})	FWHM (cm^{-1})	Intensity (arbitrary units)
850	264.5	17.3	122	284.1	9.0	27.5
875	264.0	20.5	138	283.3	8.5	27.2
900	263.0	19.8	146	282.9	8.1	25.1
925	262.1	19.2	119	280.6	5.0	14.5
950	260.2	19.5	162	276.8	7.0	11.2

Annealing temperature (°C)	AlAs-like TO mode Peak (cm^{-1})	FWHM (cm^{-1})	Intensity (arbitrary units)	AlAs IF/LO mode Peak (cm^{-1})	FWHM (cm^{-1})	Intensity (arbitrary units)
850	358.8	11.7	62.1	382.6	16.9	13.7
875	358.8	11.7	68.8	378.7	17.5	19.2
900	358.5	12.8	70.8	379.9	19.1	20.6
925	359.3	14.4	71.0	380.5	16.5	28.9
950	357.6	15.2	72.4	378.8	15.6	40.7

as this can be a useful tool to provide feedback for process development. Plots of the Raman features that show clear trends with annealing temperature, and therefore intermixing, are given in Fig. 4. The GaAs-TO peak and the GaAs IF to TO intensity ratio have the most reliable and clearest trend as a function of annealing temperature. The other parameters shown give clear monotonic shifts for the higher degrees of intermixing, but would not allow the 850 and 875 °C samples to be reliably distinguished in this data set. With the reliable shifts of the GaAs modes, we can distinguish between increases or decreases in QWI due to changes in process parameters, and we can distinguish different degrees of intermixing across different spatial regions of an intermixed structure, provided the regions are comparable to the spot size used.

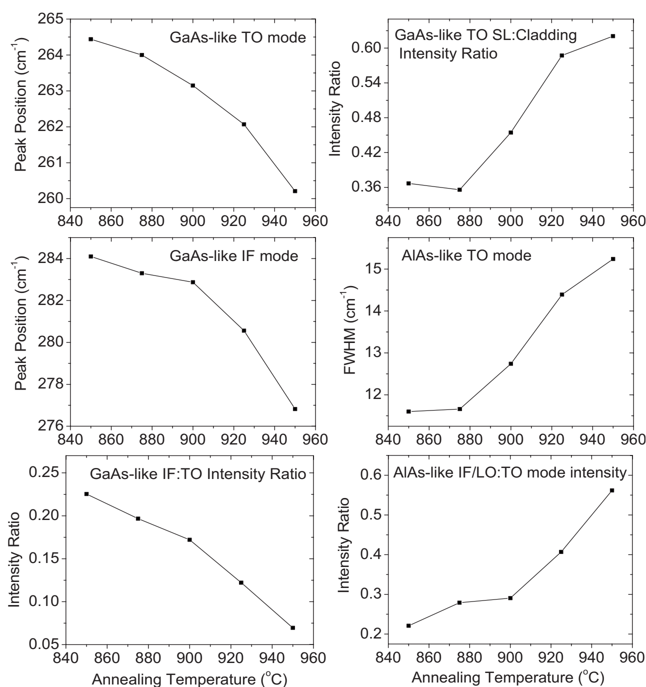

FIG. 4. Raman spectral features with clear trends vs. annealing temperature.

In order to better see the correlation between the Raman features and the PL shifts, we plotted the Raman shifts versus PL wavelength for the GaAs-like TO mode and the GaAs IF:TO intensity ratio in Figs. 5(a) and 5(b). As can be seen, these parameters exhibit a nearly linear relation with the PL wavelength. It is instructive to note that the PL wavelength, for the highest annealing temperature, namely 950 °C, does not correspond to complete intermixing in the SL. This is

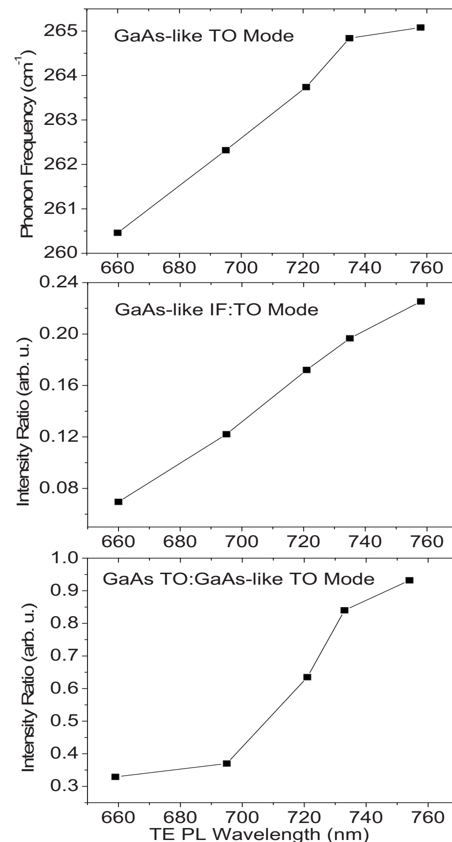

FIG. 5. The shifts of (a) the GaAs-like TO peak position and (b) the GaAs-IF mode vs. the TE polarized PL wavelength, and (c) the intensity ratio of the GaAs-like alloy and bulk-like modes.

Author complimentary copy. Redistribution subject to AIP license or copyright, see http://jap.aip.org/jap/copyright.jsp

achieved at a wavelength of 598 nm as seen for fully intermixed SL in the previous section. Linearly extrapolating the Raman shifts plotted in Figs. 5(a) and 5(b) down to the fully intermixed wavelength is not possible. The IF:TO ratio is approaching zero and the GaAs TO peak position is already near that for completely intermixed material, so to distinguish further intermixing than the one achieved for annealing temperature is not possible using this route. However, the relative intensity of the bulklike GaAs peak, at 268 cm^{-1}, which is still evident in the spectra from the 950 °C sample, may be weighted against the alloy peak to indicate further intermixing. To illustrate this, the GaAs and GaAs-like TO peaks were individually fit and their intensity ratio was plotted versus the PL wavelength [Fig. 5(c)]. (For a reliable fit, it was necessary to separately fit the GaAs DA mode.) The trend is not as clear as for the previous parameters, but this plot provides a promising route to further detect intermixing after the GaAs IF mode is indistinguishable and the position of the dominant GaAs-like TO peak is already that of 50% Al alloy.

C. Bandgap grating samples

The ability to resolve different degrees of intermixing by scanning the Raman probe laser along the [110] direction while the laser spot lies in the center of the SL layer has also been examined. This was carried out for a sample with a periodic bandgap grating fabricated using ion implantation (sample 8). The grating was designed to have a period of 3.8 μm with a 50% duty cycle, although ion straggle and defect diffusion will cause a variation on this cycle. The laser spot was centered on the SL layer, and subsequent spectra were taken at steps of 0.1 μm as the probe was scanned across several cycles of the grating period.

The shift in position of the GaAs-like TO peak corresponds to that anticipated from measurement of the large area samples, providing a strong contrast between intermixed and intermixing suppressed regions. The peak value on the intermixing suppressed region corresponds closely to the bulk like GaAs-TO peak seen at 268 cm^{-1}, and the peak on the intermixed region matches that expected for $Al_{0.5}Ga_{0.5}As$ at 260.8 cm^{-1}.[24,23] This provides a clear indication of the degree of intermixing in both regions of the grating, which in this case appears to alternate between intact SL and the equivalent bulk AlGaAs. The AlAs-like TO and LO modes were detected, but due to their limited dispersion with Al composition and poor signal ratio, respectively, their modulation was much less pronounced, being on the order of 1 cm^{-1} between the intermixed and intermixing-suppressed regions.

In Figs. 6(a) and 6(b), the wavenumber and area under the peak for the GaAs-like TO mode are plotted as a function of position along the bandgap grating. In addition, Fig. 6(c) shows the area underneath the GaAs IF mode. It is clear that the peaks are not resolved where the sample is intermixed, and thus provide a superior SNR for detecting the SL intermixing along the grating in comparison to the evidence provided from the GaAs-like TO mode. Also shown for comparison are the clearest parameters of the AlAs modes [Figs. 6(e) and 6(f)], which fail to provide as clear an SNR as the GaAs mode parameters. The scan of the PL is provided in Fig. 6(d) to correlate with the Raman modes. The PL peak takes on a value of 757 nm in the as-grown SL region, comparing with 752 nm on the large area as-grown SL sample. This inconsistency is within the PL spread across the wafer. In the center of the intermixed region, the PL peak is at 682 nm. This compares poorly with the 598 nm peak seen on the fully intermixed sample, and suggests incomplete intermixing of the SL in at least part of the intermixed grating region. The absence of the 598 nm peak in the PL may arise due to photogenerated carrier diffusion to an incompletely intermixed region with the smaller 682 nm bandgap. The PL scan does in fact show evidence of carrier diffusion, as the regions of lower bandgap appear notably larger than those of higher bandgap. This gives the false impression of an asymmetric duty cycle between the intermixed and intermixing-suppressed regions. The Raman profiles give a closer correspondence to the structural profile since Raman does not rely on carriers. From Figs. 6(a)–6(c), it can be seen that the duty cycle of the bandgap grating is close to 50 % as designed.

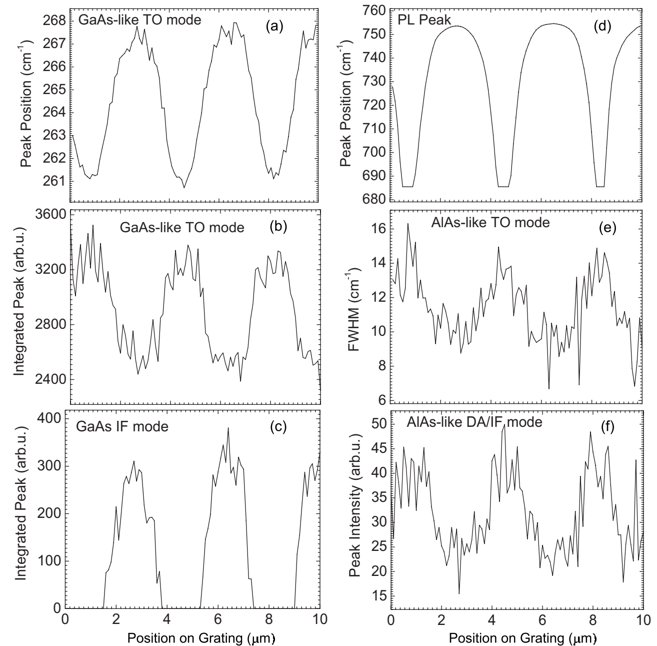

FIG. 6. Profiles along the bandgap grating at the SL core layer are shown, revealing the (a) GaAs-like TO mode position, (b) GaAs-like TO mode integrated area, (c) GaAs-like IF TO mode integrated area, (d) PL peak position, (e) AlAs-TO FWHM, and (f) the AlAs-like DA/IF mode integrated area.

Inconsistency seems to arise in the Raman spectra where no IF modes could be observed are correlated with those of the PL at 682 nm, which suggest incomplete intermixing of the SL. The answer lies in the fact that a weak IF mode Raman signal from a small incompletely intermixed region can be buried under the tail of the GaAs-like TO mode, even while the region produces a strong PL signal.

V. SUMMARY

In summary, Raman modes were used to characterize intermixing of GaAs:AlAs SL structures through spatially

Author complimentary copy. Redistribution subject to AIP license or copyright, see http://jap.aip.org/jap/copyright.jsp

resolved Raman spectroscopy. The intermixing was observed to degrade the IF mode, which can be used as a sensitive indicator of the quality of the SL and lead to the formation of interfacial alloy regions resulting in the appearance of a GaAs-like TO alloy mode distinct from the GaAs-TO bulk mode. These features, along with spatially resolved PL, were used to investigate the bandgap modulation in a periodically intermixed grating fabricated in this SL structure. Due to the large contrast they exhibit between intact and intermixed SL material, IF modes are promising for characterizing III-V SL structures that rely on intricate bandgap features defined by QWI or otherwise and particularly when COP modes are not distinguished.

[1]S. Wagner, B. M. Holmes, A. S. Helmy, D. C. Hutchings, and J. S. Aitchison, IEEE Photon. Technol. Lett. (in press).
[2]P. Dumais, A. Villeneuve, A. S. Helmy, J. S. Aitchison, L. Friedrich, R. A. Fuerst, and G. I. Stegeman, Opt. Lett. **25**, 1282 (2000).
[3]A. S. Helmy, D. C. Hutchings, T. C. Kleckner, J. H. Marsh, A. C. Bryce, J. M. Arnold, C. R. Stanley, J. S. Aitchison, C. T. A. Brown, K. Moutzouris, and M. Ebrahimzadeh, Opt. Lett. **25**, 1370 (2000).
[4]E. H. Li, E. S. Koteles, and J. H. Marsh, IEEE J. Sel. Top. Quantum Electron. 4 (1998).
[5]A. S. Helmy, A. C. Bryce, D. C. Hutchings, J. S. Aitchison, and J. H. Marsh, J. Appl. Phys. **100**, 123107 (2006).
[6]K. Zeaiter, D. C. Hutchings, K. Moutzouris, S. V. Rao, and M. Ebrahimzadeh, Opt. Lett. **28**, 911 (2003).
[7]A. Gustafsson, M. E. Pistol, L. Montelius, and L. Samuelson, J. Appl. Phys. **84**, 1715 (1998).
[8]S. Wagner, A. Al Mehairy, J. S. Aitchison, and A. S. Helmy, IEEE J. Quantum Electron. **44**, 424 (2008).
[9]G. Abstreiter, E. Bauser, A. Fischer, and K. Ploog, Appl. Phys. A: Mater. Sci. Process. **16**, 345 (1978).
[10]B. Jusserand and M. Cardona, *Light Scattering in Solids V* (Springer-Verlag, Berlin, 1989), Chap. 3.
[11]B. Jusserand, F. Alexandre, D. Paquet, and G. Le Roux, J. Appl. Phys. **47**, 301 (1985).
[12]G. Zanelato, Y. A. Pusep, J. C. Galzerani, D. I. Lubyshev, and P. P. Gonzalez-Borrero, Physica E (Amsterdam) **10**, 587 (2001).
[13]A. S. Helmy, A. C. Bryce, C. N. Ironside, J. S. Aitchison, and J. H. Marsh, Appl. Phys. Lett. **74**, 3978 (1999).
[14]P. Scrutton, M. Sorel, D. C. Hutchings, J. S. Aitchison, and A. S. Helmy, IEEE Photon. Technol. Lett. **19**, 677 (2007).
[15]C. Colvard, T. A. Gant, M. V. Klein, R. Merlin, R. Fischer, H. Morkoc, and A. C. Gossard, Phys. Rev. B **31**, 2080 (1985).
[16]S. K. Yip and Y. C. Chang, Phys. Rev. B **30**, 7037 (1984).
[17]A. K. Sood, J. Menendez, M. Cardona, and K. Ploog, Phys. Rev. Lett. **54**, 2115 (1985).
[18]B. K. Ridley, Phys. Rev. B **47**, 4592 (1993).
[19]C. Trallero-Giner, F. Garcia-Moliner, V. R. Velasco, and M. Cardona, Phys. Rev. B **45**, 11944 (1992).
[20]M. P. Chamberlain, M. Cardona, and B. K. Ridley, Phys. Rev. B **48**, 14356 (1993).
[21]M. Zunke, R. Schorer, G. Abstreiter, W. Klein, and G. Weimann, Solid State Commun. **93**, 847 (1995).
[22]O. K. Kim and W. G. Spitzer, J. Appl. Phys. **50**, 4362 (1979).
[23]D. J. Lockwood and Z. R. Wasilewski, Phys. Rev. B **70**, 155202 (2004).
[24]S. Baroni, P. Giannozzi, and E. Molinari, Phys. Rev. B **41**, 3870 (1990).
[25]D. C. Hutchings, IEEE J. Sel. Top. Quantum Electron. **10**, 1124 (2004).
[26]M. P. Chamberlain, Phys. Rev. B **48**, 11863 (1993).
[27]D. C. Hutchings and T. C. Kleckner, J. Opt. Soc. Am. B **19**, 890 (2002).

Author complimentary copy. Redistribution subject to AIP license or copyright, see http://jap.aip.org/jap/copyright.jsp